16TH INTERNATIONAL SYMPOSIUM ON BALLISTICS
SAN FRANCISCO, CA, 23-28 SEPTEMBER, 1996

SIMULATION OF A CERAMIC IMPACT EXPERIMENT USING THE SPHINX SMOOTH PARTICLE HYDRODYNAMICS CODE

D. A. Mandell, C. A. Wingate, and L. A. Schwalbe
Los Alamos National Laboratory, Los Alamos, New Mexico 87545

We are developing statistically based, brittle-fracture models and are implementing them into hydrocodes that can be used for designing systems with components of ceramics, glass, and/or other brittle materials. Because of the advantages it has simulating fracture, we are working primarily with the smooth particle hydrodynamics code SPHINX. We describe a new brittle fracture model that we have implemented into SPHINX, and we discuss how the model differs from others. To illustrate the code's current capability, we simulate an experiment in which a tungsten rod strikes a target of heavily confined ceramic. Simulations in 3D at relatively coarse resolution yield poor results. However, 2D plane-strain approximations to the test produce crack patterns that are strikingly similar to the data, although the fracture model needs further refinement to match some of the finer details. We conclude with an outline of plans for continuing research and development.

INTRODUCTION

Brittle materials are used in many defense applications. Certain armors have ceramic elements, for example. Underground bunkers consist of rock and concrete, and windshields in trucks, jeeps, and helicopters are made of glass. Any hydrocode used in the design or in the performance assessment of systems like these must accurately model the strength and fracture properties of brittle materials. The results of a hydrocode simulation depend on several factors including the particular way its fracture model is implemented. In general, fracture models must be tailored to the type of code–Lagrangian, Eulerian, or smooth particle hydrodynamics (SPH)–so that physically realistic cracks result in the context of the code's numerical treatment. But even the same model, implemented into two hydrocodes of the same type but with different coding details, can produce different results.

Statistical fracture models incorporate a number of features including 1) the introduction of a random distribution of flaws, 2) a differential equation for evolving the local damage variable, 3) formulas for degrading the material strength, for modifying the equation of state (EOS), and for relaxing the stress components of the damaged material, and 4) methods for producing and representing cracks in the computational mesh. All of these components are interdependent and must function in mutually compatible ways if the experiments are to be modeled accurately.

We have chosen to use SPHINX for the present studies. SPHINX is based on the smooth particle hydrodynamics (SPH) formalism, which has certain advantages over other methods for modeling fracture. For example, once the damage is calculated and the material properties degraded, SPH allows for the natural insertion of voids. SPH offers several additional benefits. Unlike conventional Lagrangian techniques, SPH avoids mesh tangling and is therefore much

more robust in its treatment of problems with large material distortions. In general, SPH is more computationally efficient than Eulerian codes, and it avoids advection problems, such as numerical diffusion. SPH does have its own set of problems including instabilities in tension[1]. Among other topics, we discuss this instability and possible methods to reduce or eliminate it.

To be useful as a design tool, a hydrocode, along with its material strength and fracture models must be able to predict a wide range of experiments. Many fracture models are able to simulate one-dimensional (1D) flyer plate experiments accurately, but are unable to predict multi-dimensional data. Some models are accurate for a restricted set of geometries and boundary and initial conditions, but not for others. Our goal, which we have not yet reached, is to provide a hydrocode-based design tool with a single model for the strength and fracture of brittle materials that will accurately simulate a wide range experiments and real applications.

The SPHINX code is well documented[2] and includes several of a number of models that have been proposed to simulate dynamic brittle fracture[3–8]. We have applied SPHINX with its Cagnoux-Glenn model[8,9] to simulate the impacts of steel projectiles on glass[10–12]. The results of the simulations agreed reasonably well with the global data, such as depth of penetration and the measurements of the free surface velocity on the backside of the target, but we were unable to match finer details of the crack patterns. Nor were we able to predict other experiments with the model parameters that were successful in the glass-impact study.

The primary subject of this investigation is an experiment that was conducted several years ago at Los Alamos in which a short tungsten rod strikes a target of heavily confined alumina[13]. We modeled the test with a newly implemented statistical fracture model[14] which we describe next.

THE FRACTURE MODEL

Statistical fracture modeling in hydrocodes is a relatively new innovation. Benz and Asphaug (BA) pioneered this field several years ago with the introduction of two models[3,4]. We began our investigations of statistical fracture with the model described in their more recent work[4], but in the process of implementing and testing the model in SPHINX, we changed it to such an extent that it is no longer fair to attribute the result to the original authors. Having acknowledged our debt to BA, we shall simply refer to our version as the smooth particle hydrodynamics statistical fracture (SPHSF) model.

The most important differences between the SPHSF model and those published by BA are the ways we seed the flaws and assign the flaw strengths or threshold stress values at which the flaws initiate damage in their local particles. BA select flaw strengths as uniform intervals on the domain of the Weibull distribution function[15,16] and assign the flaws to randomly selected particles. BA continue the process of assigning flaws to particles until every particle contains at least one flaw. In SPHSF, we begin with an empirical parameter that defines the average number of flaws per unit volume. We then calculate the number of flaws in each particle from a Poisson distribution[17] using the particle volume and the average flaw density. We adopted the new approach to avoid having the final distribution of flaws depending on the spatial resolution of the problem. (Although to spare computer memory, we typically limit number of flaws in each particle to the ten weakest.)

In principle, once the flaws are seeded we could use any statistical distribution for assigning their strengths. However, we follow the precedent set by BA and use the Weibull distribution

although we use a slightly different functional form. We define the distribution as

$$P(\sigma) = 1 - \exp\left(-\frac{V}{V_o} n(\sigma) \right) \quad , \tag{1}$$

where V is the volume of the sample, and V_o is the average sample size per flaw so that the total number of flaws in the material $N = V/V_o$. The function $n(\sigma)$ in Eq. 1 is defined as

$$n(\sigma) = \left(\frac{\sigma - \sigma_u}{\sigma_o} \right)^m \quad . \tag{2}$$

where m, σ_u and σ_o are parameters that characterize intrinsic properties of the material and are independent of the sample volume. The variable σ is a critical stress at which a given flaw begins to accumulate damage to the particle in which it resides. With these definitions, we interpret Eq. 1 as follows: In the limit of large N, $NP(\sigma)$ is the number of flaws in a sample of volume V that have critical stresses less than or equal to σ.

Besides using a different functional form for the Weibull distribution, we also differ from BA in the way we use the distribution. Instead of defining stresses as uniform intervals on the domain, we use a random number generator to select from the full distribution. We show elsewhere[14] how this approach reproduces the expected distribution of the weakest flaw in a collection of samples. The form of Eqs. 1 and 2 is also consistent with the observations that larger samples (those with larger V) are more likely to break.

The remaining aspects of the SPSF model are fairly standard. As we mentioned above, each flaw activates damage when the maximum principal stress in the local particle exceeds the flaw's assigned threshold. We define a scalar damage variable D for each particle as the fraction of its volume that is relieved of stress by the growing cracks. SPHINX evolves the damage variable with the ordinary differential equation,

$$\frac{dD^{1/3}}{dt} = n_i \frac{C_g}{R_s} \quad , \tag{3}$$

which is very similar to the one BA use[4]. In Eq. 3, n_i is the number of active flaws for particle i, C_g is the speed at which the crack grows, which we take as a constant equal to 0.4 times the sound speed, and R_s is a characteristic length. We use the cube root of the particle volume for the characteristic length.

Once we compute the damage, we have to couple it back to the material strength and hydrodynamics calculations. The current version of SPHINX allows us to scale the yield stress and/or shear modulus for each particle linearly between a value corresponding to the intact material and a value corresponding to the fully fractured material. In this work, we use a constant shear modulus and let the yield stress decrease linearly to zero as the damage increases from zero to one. Other authors take different approaches. For example, Benz and Asphaug do not modify their calculation of the stress deviators. Instead, they include a factor of 1 – D in the equations where the stress deviators are used. Randles and coworkers[6] modify the bulk modulus and the yield strength in tension only by a factor of $1 - D_t^2$, where D_t is the tensile damage parameter. The latter authors also include shear damage in their model.

Finally, the codes must have a way to let the particles separate and form cracks and material fragments. Again, different researchers use different methods to achieve particle separation. If a particle is fully damaged (D = 1.0), BA exclude that particle from the SPH summations over the neighboring particles. This exclusion effectively disconnects the damaged particle from its neighbors.

Other methods have been used to produce crack structures. Randles and coworkers[6] disconnect their damaged particles by reducing the smoothing length h. To prevent adverse effects on the time step, they limit the reduction of h to 0.8 of its original value. SPHINX can use either of these two methods. In this work, we use the sum exclusion method, but we do so only when the sum of the pressures of the damaged particle and that of its neighbors is negative. This scheme allows damaged particles to resist compression but not tension.

ROD IMPACT INTO A HEAVILY CONFINED CERAMIC

To illustrate the utility of the SPHSF model in SPHINX, we simulated the impact of a short, tungsten rod with a hemispherical nose into a cylindrically shaped target of heavily confined alumina AD85[13] (see Fig. 1). The rod was approximately 1.8 cm long and 0.4 cm in radius and had an initial velocity of 1.288 km/s. The alumina was about 9 cm long and 5 cm in diameter.

We used linear U_s-U_p equations of state (EOS) and elastic/perfectly plastic strength models for all materials in the problem. Table 1 summarizes the constants used for the ceramic in each of the calculations described below. The first seven entries are standard input for the EOS and strength models in SPHINX[2] and are reasonably well defined. The last four entries are parameters for the Poisson and Weibull distributions that characterize the fracture.

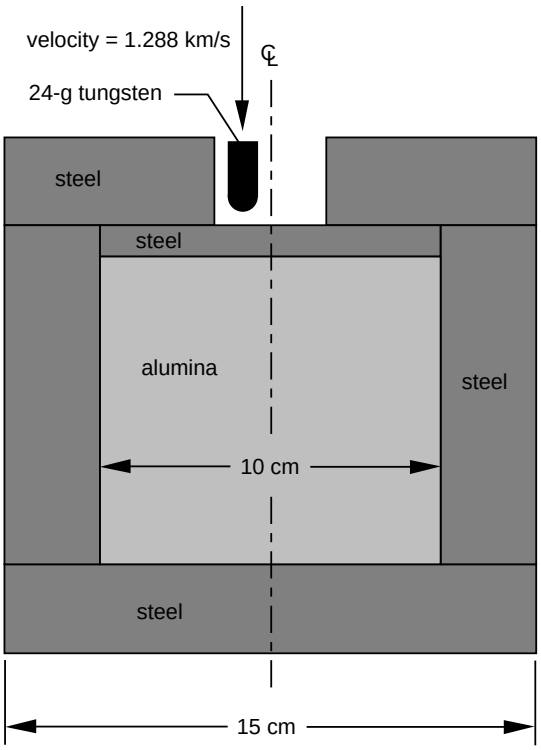

Fig. 1 Schematic cross section of the test configuration.

PARAMETER	VALUE
ρ (material density)	3.41 g/cm^3
c (sound speed)	0.819 x 10^6 cm/s
s (U_s–U_p slope)	0.88
γ0	0.0
γ1	1.24
Y_o (yield stress)	150.0 kbar
μ (shear modulus)	1.869 Mbar
σ_o	20.0 kbar
σ_u	0.0 kbar
m	10
flaw density	500/cm^3

Table 1. Equation-of-state, strength, and fracture parameters for the AD85 alumina.

The fracture constants for AD85 alumina are not well defined. Ideally, for a problem like this, we would use parameters that had been established from an independent set of calibrations. For example, we might have used quasi-static, uniaxial strain measurements to find the constants for the statistical distribution of the flaw strengths (Eqs. 1 and 2) as Weibull described[15]. But we had no data of this sort available, and so we estimated a set of constants based, in part, on data presented in Weibull's paper and on what we know (or can guess) about the experiment itself. Given this self-consistent approach to find appropriate values for the fracture constants, our calculations are better described as "models" of the experiment rather than as "predictions." Among our plans for continuing research, we hope to explore ways of independently calibrating the constants in our models, and we must also examine the sensitivities of our predicted results to the precisions of these parameters.

Figure 2 shows a cross section of the target after the test was run. To facilitate handling, most of the target's radial confinement was cut away, and the interior portion was sectioned and stained with a dye penetrant to reveal the cracks. Our first attempt to simulate the test was a fully three-dimensional (3D) model using 342,989 particles. Figure 3 shows a a cut-away view of the ceramic portion of the target at late time (100 μs). The lighter gray regions mark the fully damaged material, and the darker grey show the intact material. Comparing Figs. 2 and 3, we see that our simulations do not reproduce the experimental crack pattern.

At the time we completed this run, we were uncertain about the reasons for the discrepancy, and we felt that we had to explore the parameter space more extensively. However, because of the size and complexity of the 3D problem, we chose to continue with a series of two-dimensional (2D), plane-strain approximations to the actual geometry. The advantage of 2D is economy: we can model the problem in 2D with higher spatial resolutions and simultaneously reduce the run times.

Fig. 2. Sectioned and stained target with parts of the radial containment removed.

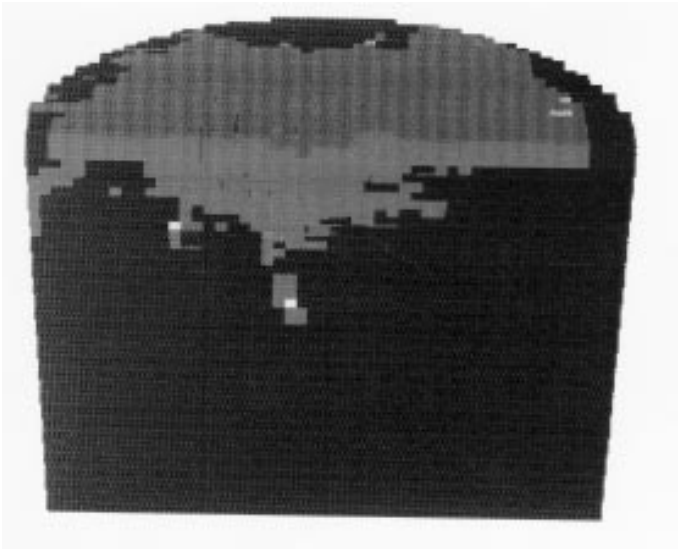

Fig. 3. Result of full 3D SPHINX simulation at 100 μs using 342,989 particles.

Figure 4 shows the result of our 2D plane-strain model. We will refer to this calculation in the following discussion as our baseline. In this run, we used 55,435 particles, which represents the equivalent spatial resolution of a 13-million-particle calculation in 3D. Once again, we ran the simulation to 100 μs, which is long enough that no further changes occur in the depth of penetration or the crack pattern. The runtime was 1.29 CPU h on 256 processors of our massively parallel T3D computer. Comparing the results in Figs. 2 and 4, we see much better qualitative agreement than we obtained in 3D. For example, the code seems to model accurately the diagonal crack structures that radiate from the impact region. However, as we expect, the simulation does not exactly reproduce all details of the experimental crack structure. Some of the finer structures do not appear at all. Moreover, the simulation underpredicted the measured depth of rod's penetration.

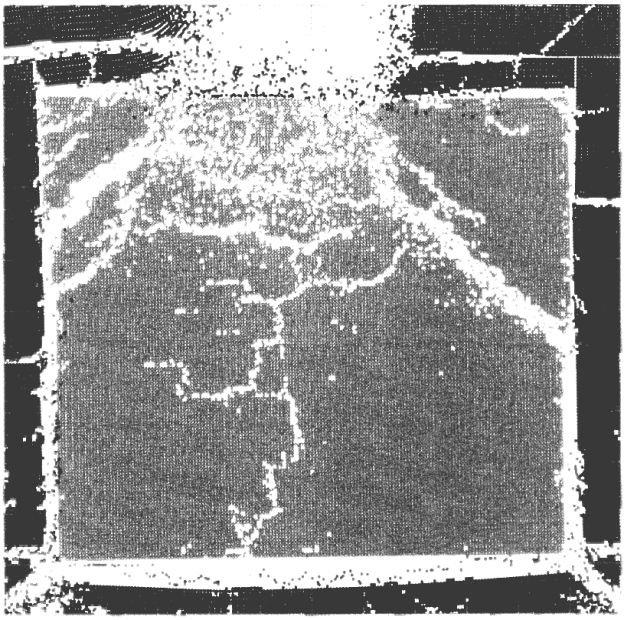

Fig. 4. Result of 2D SPHINX simulation at 100 μs using 55,435 particles.

To study the effects of changes in the spatial resolution, we repeated the baseline calculation, first, with roughly half the number of particles and, second, with roughly double the number. Figures 5 and 6 show the results of these runs at 100 μs. Comparing Figs. 4 and 5, we see that the lower-resolution result omits many of the important crack features. The crack pattern from the higher-resolution model (Fig. 6) is qualitatively similar that obtained from the baseline.

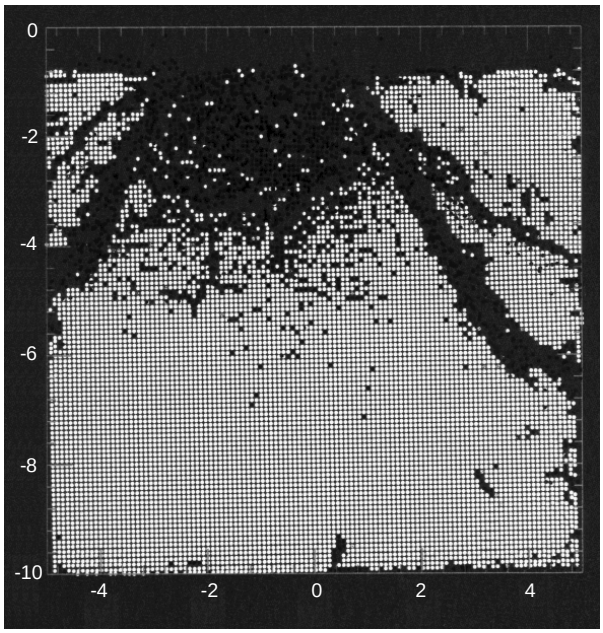

Fig. 5. Result of 2D SPHINX simulation at 100 μs using 27,638 particles. The scale of the plot is in cm.

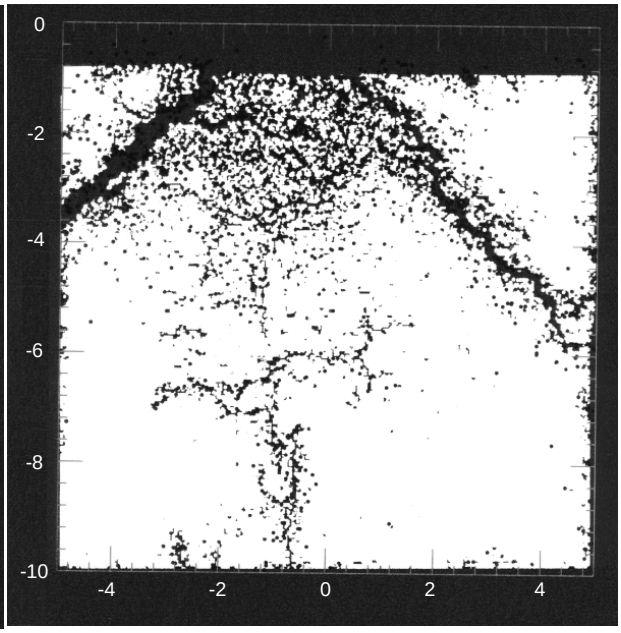

Fig. 6. Result of 2D SPHINX simulation at 100 μs using 100,769 particles. The scale of the plot is in cm.

One implication of the 2D mesh-convergence study is that we are not calculating the correct crack pattern in 3D because we did not resolve the problem well enough. Among our plans for continuing research are to produce 3D calculations with more particles and also to investigate better ways of distributing the particles.

The baseline calculation in Fig. 4, had the SPHSF model operating in all of the materials. It is interesting to compare this result with a calculation in which fracture is allowed only in the ceramic. The result, which we present in Fig. 7, shows all of the major features of the crack pattern exhibited by the baseline. Only a few details are different.

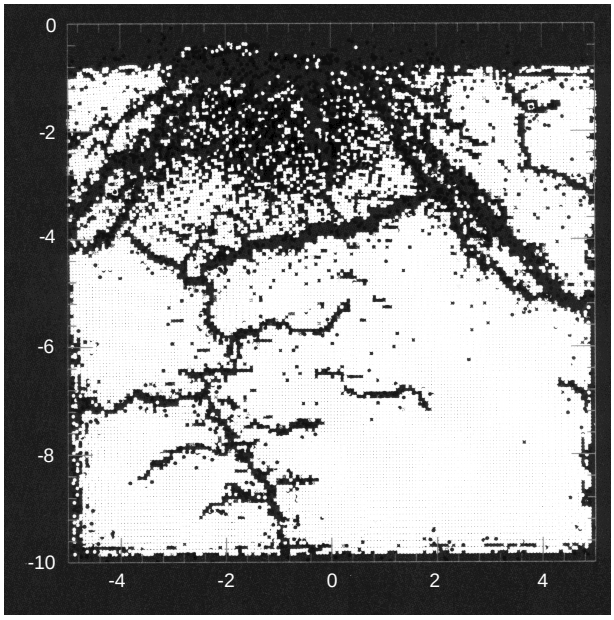

Fig. 7. Repeat of the baseline calculation with the fracture model operating in the ceramic region only. The scale of the plot is in cm.

To examine the effect of removing the mechanism in the SPHSF for opening cracks, we repeated our baseline run with the disconnect option turned off. We observed no cracks in the ceramic even though a color plot of the damage (not shown) indicates that more damage occurred in this case than in the corresponding baseline calculation. We conclude from this comparison that to see correct crack patterns form, it is essential that we disconnect fully damaged SPH particles from their neighbors and allow the local stress fields to relax.

We must include a few comments in closing about the tensile instability problem[1] that has yet to be solved. SPHINX and other SPH codes exhibit a numerical instability in regions of tension that tends to bunch particles together. The instability is a fundamental problem with the SPH method and is particularly worrysome for those of us who study fracture because it can produce artificial crack structures that look very convincing. We try to avoid drawing conclusions from results that may have been caused by this artifact by running parallel problems with and without the fracture model. Specifically, for the present case, we satisfied ourselves that our SPHSF model is producing the crack structures because we observed no damage without the model.

In our broader experience, the effects of the tensile instability are somewhat problem dependent and are mitagated somewhat by the reduction of the tensile pressure due to the damage, as BA have discussed[3]. Moreover, as we and others have observed, the instability problem can be significantly reduced by including more particles in the SPH sums–mathematically, we accomplish this by increasing the initial smoothing length for each particle by a factor of 1.5 or more. We used this method in the present work.

So far our attempts to avoid or reduce the effects of the instability have been no more than *ad hoc* fixes. Some researchers have proposed algorithms to eliminate the problem with a staggard mesh scheme[18], but these approaches have not yet been demonstrated in 2D and 3D. Wen and coworkers[19] have proposed the method of conservative smoothing that we have implemented into SPHINX along with a related method that we call local conservative smoothing. We are currently testing both algorithms. Preliminary results indicate that conservative smoothing does improve the results of some problems but is not a complete solution for all cases.

FUTURE WORK

We mentioned in the discussion some of the plans we have for continuing research. The most important objective is to extend this study to 3D. As an intermediate step toward this goal, we hope to conduct some studies in 2D axisymmetric geometry. We have not begun this work because the 2D axisymmetric option is not available yet in the T3D-version of SPHINX. We will also continue studying the sensitivities of damage to the various parameters in our model. In terms of improving the SPHSF model itself, we are currently calculating material damage through tensile forces only, but we recoginze the importance of shear stresses in the fracture process[6,20], and we intend to include the effects of shear in SPHSF at some point. Also, our model uses a scalar damage variable. Randles and Libersky[7] have proposed using instead a tensor damage variable D_{ij}, which should be more physically realistic. We hope to include this refinement as well as some of these authors' other suggested improvements, such as internal boundary conditions on crack surfaces, for example. Finally, we are continuing our research to eliminate the tensile instabilities, and we are applying the new model to other test data.

REFERENCES

1. J. W. Swegle, D. L. Hicks, and S. W. Attaway, "Smoothed Particle Hydrodynamics Stability Analysis," J. Comput. Phys., 116, 123, (1995).
2. C. A. Wingate, and R. F. Stellingwerf, Los Alamos SPHINX Manual Version 7.6, Los Alamos National Laboratory Report LAUR 93-2476 (March 8, 1995).
3. W. Benz, and E. Asphaug, "Impact Simulation with Fracture: I. Methods and Tests," ICARUS, 107, 98, (1994).
4. W. Benz, and E. Asphaug, "Simulations of Brittle Solids Using Smooth Particle Hydrodynamics," Computer Physics Communications, 87, 253, (1995).
5. G. R. Johnson, and T. J. Holmquist, "A Computational Model for Brittle Materials Subjected to Large Strains, High Strain Rates, and High Pressures, in Shock-Wave and High-Strain-Rate Phenomena in Materials," ed. by Marc A. Meyers, Lawrence E. Murr, and Karl P. Staudhammer, Marcel Dekker, Inc., New York (1992).
6. P. W. Randles, T. C. Carney, and L. D. Libersky, "Continuum Dynamical Simulations of Bomb Fragmentation," Proceeding of the 15th International Symposium on Ballistics, Jerusalem, Israel, (May 21-24, 1995).
7. P. W. Randles, and L. D. Libersky, "Smoothed Particle Hydrodynamics: Some Recent Improvements and Applications," Computer Methods in Applied Mechanics and Engineering (in press, 1996).
8. J. Cagnoux, "Modele Phenomenlogique D'Ecaillage D'Un Pyrex" (Phenomenological Model of Spalling of Pyrex Glass), Journal De Physique, Colloque C5, supplement au n^{o}8 Tome 46, (1985).
9. L. A. Glenn, B. Moran, and A. Kusubov, "Modeling Jet Penetration In Glass," Conference on the Application of 3-D Hydrocodes to Armor/Anti-Armor Problems, Ballistic Research Laboratory, Aberdeen Proving Grounds, MD, (May, 1990).

10. D. A. Mandell, and C. A. Wingate, "Numerical Simulations of Glass Impacts Using Smooth Particle Hydrodynamics," 1995 APS Topical Conference on Shock Compression of Condensed Matter, Seattle, WA (August 13-18, 1995).

11. D. A. Mandell, C. A. Wingate, R. F. Stellingwerf, "Prediction of Material Strength and Fracture of Brittle Materials Using the SPHINX Smooth Particle Hydrodynamics Code," Proceedings of the 10th ASCE Engineering Mechanics Conference, Boulder, CO, (May 21-24, 1995).

12. R. J. Henninger, D. A. Mandell, R. A. Huyett, and F. S. Lyons, "Improvement of Glass-Plastic Transparent Armor Using Computational Modeling," Sixth Annual US TARDEC Combat Vehicle Survivability Symposium, Monterey, CA (March 28-30, 1995).

13. M. W. Burkett, and D. A. Rabern, "Stress Fields Generated by Kinetic Energy Projectile Interaction With Ceramic Targets," Shock Compression of Condensed Matter, ed. by S. C. Schmidt, R. D. Dick, J. W. Forbes, and D. G. Tasker, 947, Elsevier Science Publishers (1992).

14. R. F. Stellingwerf and L. A. Schwalbe, "Statistical Fracture Models For Smooth Particle Hydrodynamics," Los Alamos Memorandum X-1(1/95)-9 (March 8, 1995).

15. W. Weibull, "A Statistical Distribution Function of Wide Applicability", J. Appl. Mech. 18, 293-297, (1952).

16. M. F. Ashby, and D. R. H. Jones, Engineering Materials 2, Pergamon Press, New York, (1988).

17. E. L. Crow, F. A. Davis, and M. W. Maxfield, Statistics Manual, Dover Publications, Inc., New York, (1960).

18. C. T. Dyka, and R. P. Ingel, "Addressing Tension Instability," Naval Research Laboratory Report NRL/MR/6384-94-7641 (December 30, 1994).

19. Wen, Y., Hicks, D. L., and J. W. Swegle, Stabilizing S.P.H. with Conservative Smoothing, Sandia National Laboratories Report SAND94-1932 (August, 1994).

20. L. G. Margolin, "Numerical Simulation of Fracture," Proceedings of the International Conference on Constitutive Laws for Engineering Materials: Theory and Application, Tucson, AZ (January 10–14, 1983).